

Nanoscale *Stolephorus* sp. powder fabrication using high-energy milling for bioactive materials in dentistry

Anastasia Elsa Prahasti^{1,A,C,D,F}, Tamara Yuanita^{2,A,B,E,F}, Retno Pudji Rahayu^{3,C,E,F}

¹ Faculty of Dental Medicine, Airlangga University, Surabaya, Indonesia

² Department of Conservative Dentistry, Airlangga University, Surabaya, Indonesia

³ Department of Oral and Maxillofacial Pathology, Airlangga University, Surabaya, Indonesia

A – research concept and design; B – collection and/or assembly of data; C – data analysis and interpretation;

D – writing the article; E – critical revision of the article; F – final approval of the article

Dental and Medical Problems, ISSN 1644-387X (print), ISSN 2300-9020 (online)

Dent Med Probl. 2024;61(4):585–592

Address for correspondence

Tamara Yuanita

E-mail: tamara.yuanita@klinikjurnal.com

Funding sources

None declared

Conflict of interest

None declared

Acknowledgements

The authors would like to thank Research Center for Physics, Indonesian Institute of Sciences, E-Layanan Sains, Jakarta, Indonesia, for scientific and technical support.

Received on January 30, 2023

Reviewed on February 19, 2023

Accepted on April 26, 2023

Published online on August 28, 2024

Cite as

Prahasti AE, Yuanita T, Rahayu RP. Nanoscale *Stolephorus* sp. powder fabrication using high-energy milling for bioactive materials in dentistry. *Dent Med Probl.* 2024;61(4):585–592. doi:10.17219/dmp/163634

DOI

10.17219/dmp/163634

Copyright

Copyright by Author(s)

This is an article distributed under the terms of the

Creative Commons Attribution 3.0 Unported License (CC BY 3.0)

(<https://creativecommons.org/licenses/by/3.0/>).

Abstract

Background. The application of natural products in dentistry has been widely explored. Anchovy (*Stolephorus* in Latin) has been examined for its bioactive content (calcium, phosphorus and fluoride) as an agent for bone stimulation and tooth development, topical fluoridation and pulp capping. Ball milling has been used to prepare calcium oxide nanoparticles from snakehead fish bone.

Objectives. The aim of the study was to reduce the particle size of *Stolephorus* sp. powder to the nanoscale using high-energy ball milling for 8, 12 and 24 h, and to analyze the optimal milling time by comparing the powder characteristics.

Material and methods. The *Stolephorus* sp. were oven-dried at 50°C for 6 h, after which the entire fish were crushed into powder. The fish powder was produced by blending the material for 5 min and passing it through a 200-mesh sieve. The remaining dried fish was blended again for 5 min until it passed through the sieve. The top-down approach to the particle size reduction was performed using high-energy milling at 3 distinct time points (8, 12 and 24 h). The characteristics of the powder were evaluated using a particle size analyzer, a Fourier-transform infrared spectrometer (FTIR) and scanning electron microscopy–energy dispersive spectroscopy (SEM-EDS).

Results. The *Stolephorus* sp. powder contained 64.50% protein, 7,420 mg/kg sodium, 28,912 mg/kg calcium, and 1,924 mg/kg magnesium. The high-energy milling process resulted in a reduction of the particle size from the microscale to the nanoscale. The analysis of the average particle size and polydispersity index indicated that 24 h of milling showed the most optimal results. Furthermore, the functional groups exhibited no significant alteration at 3 milling times ($p \geq 0.05$, FTIR analysis).

Conclusions. The high-energy milling method has the potential to reduce the particle size of *Stolephorus* sp. powder to the nanoscale at the 8- and 24-h milling periods. The powder resulting from the 24-h milling process had a size of 789.3 ± 170.7 nm, smooth size distribution, good size uniformity, a polydispersity index of 0.763, no significant change in organic and inorganic compound content, and a calcium/phosphorus ratio that was the closest to that of hydroxyapatite (HAp).

Keywords: nanoparticle, high-energy ball milling, good health and well-being, particle size reduction, *Stolephorus* sp.

Introduction

The development of new drugs is a long process, especially for those derived from natural products. However, natural products and traditional medicine have advantages in terms of diversity of chemical structures, biological activities and clinical experience.¹ The use of natural products has been widely explored in the field of dentistry. Anchovy (*Stolephorus* in Latin) has been studied for its bioactive content (calcium, phosphorus and fluoride) as an agent for bone stimulation and tooth development, topical fluoridation, and pulp capping.² *Stolephorus* sp. is classified within the order Clupeiformes, the Engraulidae family. It is a small pelagic fish, categorized as a renewable resource, with a maximum length of 40–145 mm. It has thin, quickly shedding scales and a silvery lateral line between its chest fin and tummy fin.³ *Stolephorus* sp. can be used by extraction or as a pure powder (simplicia).² The *Stolephorus* sp. extract has superior activity compared to the pure powder in many compounds, whereas the pure powder has advantages in the number and complexity of bioactive compounds that work together.

Stolephorus sp. has been examined for its ability to increase hemoglobin levels in adolescent anemia.⁴ The calcium and amino acid content of *Stolephorus* sp. is believed to play a role in the repair of cells and could benefit the field of dentistry. Calcium is also present in other foods, such as milk, bone soup, green vegetables, beans, tofu, and tempeh. Unfortunately, the content of fiber, phytic acid and oxalic acid in other food products inhibits the absorption of calcium. In addition, the lactose content of milk limits its consumption, particularly among individuals with lactose intolerance.⁵

It has been reported that *Stolephorus* sp. increases the proliferation of odontoblasts.⁶ Another study mentioned its protein/amino acid benefits in bone function modulation.⁷ Studies on the application of *Stolephorus* sp. cream to dental pulp perforation have demonstrated that the bioactive compound of *Stolephorus* sp. escalated the formation of reparative dentin compared to calcium hydroxide application.⁸ Although, calcium hydroxide has been the gold standard for vital dental pulp perforation for decades. These findings indicate the potential for a new drug candidate for reparative dentin induction.

This study was considered necessary due to the increased success of vital pulp therapy using natural materials of nanosize to increase their effectiveness. The use of calcium hydroxide as the gold standard for vital pulp therapy is associated with the disadvantage of reparative dentin, which results in tunnel defects that lead to micro-leakage and can cause permanent pulp inflammation.^{4,5} Previous studies have shown the potential of *Stolephorus* sp. powder to stimulate the growth of odontoblasts and produce reparative dentin, exhibiting superior efficacy compared to calcium hydroxide.^{6,8} Our study aims to evaluate the technique for obtaining the nanosized *Stolephorus* sp.

powder using high-energy milling. The results obtained at 8-, 12- and 24-h were compared according to the test characteristics.

Ball milling has been used to prepare calcium oxide nanoparticles from snakehead fish bone.⁹ Previous studies have employed a chemical refining process, followed by calcination using a furnace and a ball milling process. In this study, ball milling was conducted on the whole fish powder that had been dried and blended without the application of any chemical processes. The duration of the milling process was modified to obtain nanoparticles.

Given the impact of nanoscale particles on the efficacy of *Stolephorus* sp., a reduction in the particle size could enhance the activity of *Stolephorus* sp. pure powder on cell targets.¹⁰ Nanoparticles are obtained through a top-down approach using high-energy milling. The aim of the study is to reduce the particle size of *Stolephorus* sp. powder to a nanoscale using high-energy ball milling for 8, 12 and 24 h, and to analyze the optimal milling time by comparing the powder characteristics.

Material and methods

Research design

The anchovies used in the experiment were obtained from the fish market in Muara Karang, Jakarta, Indonesia, and identified as *Stolephorus* sp. by the Indonesian Institute of Sciences, Jakarta, Indonesia (ID No. 29825). The fish were oven-dried at 50°C for 6 h,⁶ ground into a fine powder using a blender and sieved.⁸ The protein, mineral and amino acid content was analyzed at PT Saraswanti Indo Genetech Laboratory (Bogor, Indonesia). Milling was conducted at the Indonesian Institute of Sciences, Physics Research Center, followed by the particle size analysis (PSA) at PT Cipta Mikro Material (Bogor, Indonesia). Fourier-transform infrared spectrometer (FTIR) and scanning electron microscopy (SEM) analyses were performed at the Forensic Laboratory Center of Indonesian National Police in Jakarta, Indonesia.

The analysis was conducted using liquid chromatography–mass spectrometry (LC-MS) (Shimadzu Corporation, Kyoto, Japan), ultra-performance liquid chromatography (UPLC) (ACQUITY Premier System; Waters Corporation, Milford, USA) and high-performance liquid chromatography (HPLC) (Waters Corporation). The eluent for LC-MS consisted of solution A (100 mM ammonium formate in water) and solution B (acetonitrile:water:formic acid, v:v:v = 95:5:0.3). The eluent for HPLC was ethanethiol. The retention times are presented in Table 1.

Sample preparation

The LC-MS, UPLC and HPLC analyses required the sample to be hydrolyzed with 6N HCl 200 µL and 40 µL

Table 1. Amino acid content of *Stolephorus* sp. powder

Parameter	Value [mg/kg]	Retention time [min]	Method
L-cysteine	9,596.42	4.17–4.87	18-12-38/MU/SMMSIG (LC-MS)
L-methionine	7,232.12	3.50–4.20	18-12-38/MU/SMMSIG (LC-MS)
L-serine	32,648.37	5.95–6.65	18-5-17/MU/SMM-SIG (UPLC)
L-glutamic acid	64,598.39	5.31–6.01	18-5-17/MU/SMM-SIG (UPLC)
L-phenylalanine	3,6112.3	2.83–3.53	18-5-17/MU/SMM-SIG (UPLC)
L-isoleucine	28,542.91	3.32–4.02	18-5-17/MU/SMM-SIG (UPLC)
L-valine	33,534.56	3.86–4.56	18-5-17/MU/SMM-SIG (UPLC)
L-alanine	33,978.35	5.19–5.89	18-5-17/MU/SMM-SIG (UPLC)
L-arginine	45,869.46	9.24–9.94	18-5-17/MU/SMM-SIG (UPLC)
Glycine	41,542.57	5.72–6.42	18-5-17/MU/SMM-SIG (UPLC)
L-lysine	40,155.18	8.49–9.19	18-5-17/MU/SMM-SIG (UPLC)
L-aspartic acid	39,802.95	5.60–6.30	18-5-17/MU/SMM-SIG (UPLC)
L-leucine	52,350.32	3.09–3.79	18-5-17/MU/SMM-SIG (UPLC)
L-tyrosine	26,236.71	3.79–4.49	18-5-17/MU/SMM-SIG (UPLC)
L-proline	24,326.38	3.57–4.27	18-5-17/MU/SMM-SIG (UPLC)
L-threonine	34,417.33	5.24–5.94	18-5-17/MU/SMM-SIG (UPLC)
L-histidine	20,571.09	8.42–9.12	18-5-17/MU/SMM-SIG (UPLC)
L-tryptophan	4,899.71	2.97–3.67	18-5-63/MU/SMM-SIG (HPLC)

LC-MS – liquid chromatography–mass spectrometry; UPLC – ultra-performance liquid chromatography; HPLC – high-performance liquid chromatography.

phenol, and dried in the oven at 112–116°C for 20–24 h. The excess HCl was wiped off and the tubes were subjected to vacuum drying. Subsequently, the derivatization of amino acids was conducted using an AccQ-Fluor Reagent Kit (Waters Corporation), followed by the separation of amino acids. Atomic absorption spectrophotometry (AAS) required the sample to be diluted with HCl and directly injected into the atomic absorption spectrophotometer.

Protein, mineral and amino acid content analysis

The protein, mineral and amino acid content was analyzed. The total protein content of the sample was determined using a semi-automated device (behrotest® Steam Distiller type S2; behr Labor-Technik GmbH, Düsseldorf, Germany) that operates based on the Kjeldahl method.¹¹ The automatic addition of NaOH and H₂O enables the steam distiller to identify the nitrogen content. The atomic absorption spectrophotometer (AA-6800; Shimadzu Corporation) was used to evaluate the mineral composition of the sample. This flame photometry tool determines the concentration of specific metals. The amino acid profile was analyzed using a mass spectrometer (ACQUITY Premier System; Waters Corporation).

Particle size analysis

A top-down approach to reduce the particle size was performed in a manner similar to that described in the referenced study, with a modification in the milling time.⁹ The *Stolephorus* sp. powder was subjected to high-energy milling for 8, 12 and 24 h, respectively. Zirconia balls were used, with a weight ratio of 1:5 between the powder and the balls. The rotational speed in the dry grinding mode was set at 100 rpm. Before and after milling, the particle size of *Stolephorus* sp. powder was measured using a particle size analyzer (Delsa™ Nano C; Beckman Coulter, Fullerton, USA). The dynamic light-scattering instrument required sample dilution, and fluctuations in scattered laser light, resulting from Brownian motion, were interpreted as the particle size.¹²

Fourier-transform infrared spectrometry

The functional groups were identified using a FTIR (Alpha II; Bruker, Billerica, USA). The examination was performed on pellet samples of potassium bromide (KBr) (99.99%) mixed with the *Stolephorus* sp. powder. The FTIR spectrum was collected at a resolution of 4 cm⁻¹ in the transmission mode (400–4,000 cm⁻¹).

Scanning electron microscopy–energy dispersive spectroscopy

Scanning electron microscopy–energy dispersive spectroscopy (SEM-EDS) (FlexSEM 1000; Hitachi Ltd., Tokyo, Japan) was used to determine the elemental composition of the material. For this examination, the samples were coated with gold. The tool was set at 10.00 kV, with a working distance of 9.8 mm and a pressure of 80.00 Pa.

Statistical analysis

One-way analysis of variance (ANOVA) was used to examine the calcium/phosphorus (Ca/P) ratio between different milling time groups. The data was obtained from 3 repetition tests and is presented as mean ± standard deviation ($M \pm SD$). The analysis was performed using the IBM SPSS Statistics for Windows software, v. 25.0 (IBM Corp., Armonk, USA). The level of significance was set at $p < 0.05$.

Results

The average particle size of *Stolephorus* sp. powder after blending and sieving was 17.41 ± 1.80 µm. The protein content was 64.5%, and the mineral evaluation identified the presence of sodium, calcium and magnesium at concentrations of 7,420 mg/kg, 28,912 mg/kg and 1,924 mg/kg, respectively. The amino acid content of *Stolephorus* sp. powder is shown in Table 1.

Three *Stolephorus* sp. powders produced at various milling times demonstrated significantly different colors and degrees of smoothness (Fig. 1).

The test was followed by particle size measurement. The conversion of particle size from $17.41 \pm 1.8 \mu\text{m}$ to $463.3 \pm 105.7 \text{ nm}$ (8-h milling), $1,365.4 \pm 161.3 \text{ nm}$ (12-h milling) and $789.3 \pm 170.7 \text{ nm}$ (24-h milling) was observed. The complete results, including the mean particle size, *SD* and polydispersity index are presented in Table 2.

The smallest mean particle size was observed in the 8-h milling sample, but the lowest polydispersity index was noted in the 12-h sample. The 24-h milling sample showed a particle size of $789.3 \pm 170.7 \text{ nm}$, with a polydispersity index of nearly 0.7 (0.763), thereby indicating the suitability of the measurement technique.

The organic and inorganic compounds present in the samples were identified through the use of the FTIR. The FTIR graphs (Fig. 2) indicated that the 3 samples produced at different milling times created a similar pattern. In addition, the graphs recorded more than 5 peaks of transmittance, which were identified as functional group compounds (Table 3).

The SEM-EDS was performed to describe the elemental content of the samples. The results of the SEM-EDS analysis are presented in Fig. 3 and Table 4.

The SEM-EDS showed the presence of significant and minor elements in the samples. Carbon, nitrogen and oxygen dominated the results, followed by calcium and phosphorus. The Ca/P ratio is a useful indicator of the presence of hydroxyapatite (HAp). The HAp reference stoichiometry was 1.67. The 24-h milling sample exhibited the Ca/P ratio most closely aligned with the reference value. However, one-way ANOVA showed no statistically significant difference between the groups ($p \geq 0.05$).

The SEM-EDS images (Fig. 4) were captured with a magnification range between $40 \mu\text{m}$ and $200 \mu\text{m}$. The images facilitate the evaluation of particle distribution patterns and particle shapes. The scanning images of the *Stolephorus* sp.

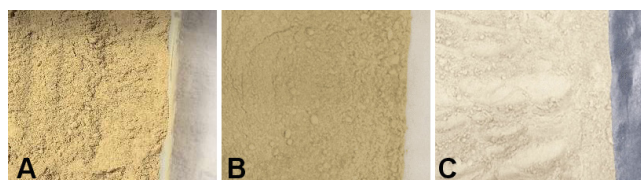


Fig. 1. *Stolephorus* sp. powders obtained at 3 milling times

A. Smooth powder with a dark color (8 h); B. More smooth powder with a darker color (12 h); C. Most smooth powder with the lightest color (24 h).

Table 2. Particle size of *Stolephorus* sp. powder at 3 milling times

Milling time	Particle size [nm] $M \pm SD$	Polydispersity index
8 h	463.3 ± 105.7	1.245
12 h	$1,365.4 \pm 161.3$	0.394
24 h	789.3 ± 170.7	0.763

M – mean; *SD* – standard deviation.

powder at 3 milling times showed that the milling time affected the particle distribution pattern. An extended milling time resulted in smoother particle distribution. Moreover, the images demonstrate that milling resulted in the formation of amorphous particles with a bumpy interface.

The changes in protein and mineral composition resulting from the milling process are shown in Table 5.

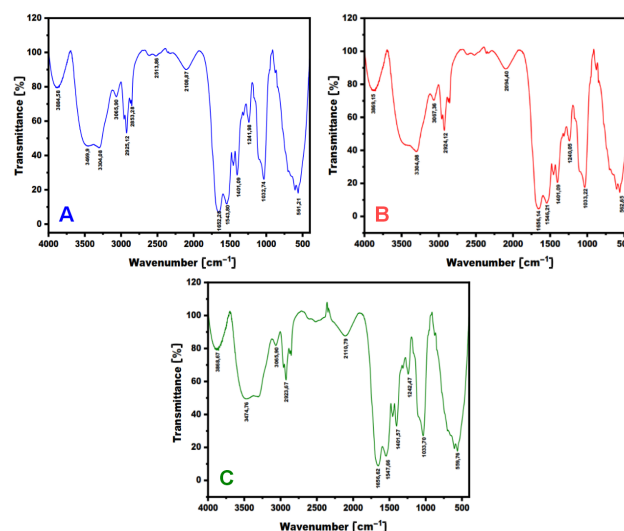


Fig. 2. Fourier-transform infrared spectrometer (FTIR) transmittance graphs of *Stolephorus* sp. powder at 3 milling times

A. 8 h; B. 12 h; C. 24 h.

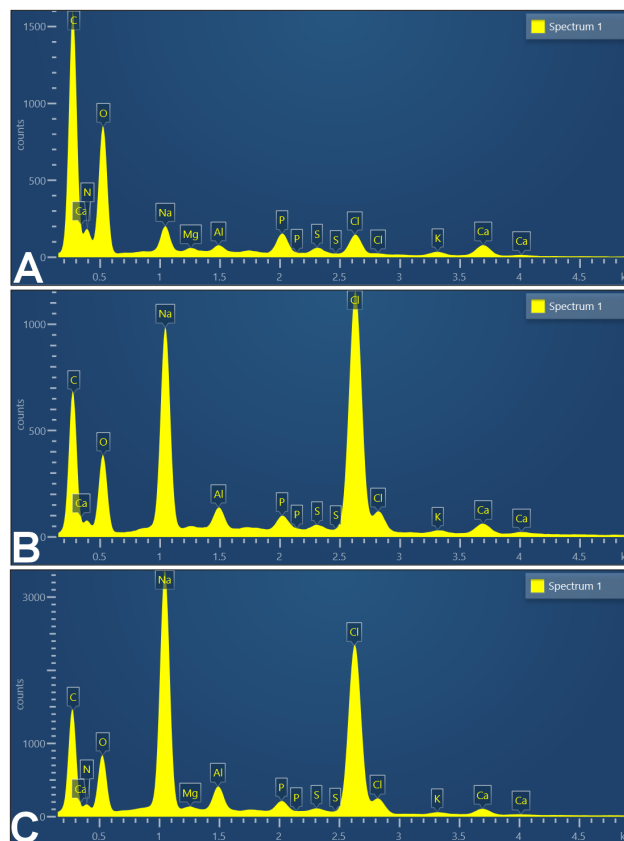


Fig. 3. Elemental spectrum of *Stolephorus* sp. powder at 3 milling times

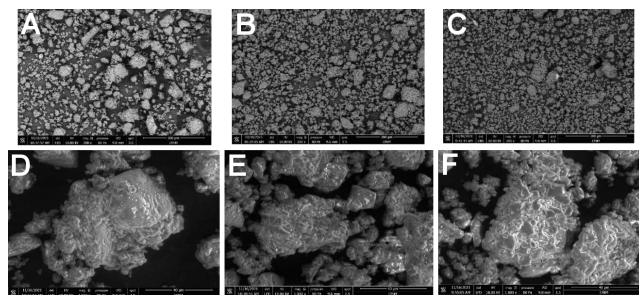
A. 8 h; B. 12 h; C. 24 h.

Table 3. Fourier-transform infrared spectrometer (FTIR) transmittance peaks of *Stolephorus* sp. powder at 3 milling times

Functional group	Wavenumber [cm ⁻¹]		
	8 h	12 h	24 h
O–H	3,884.58	3,869.15	3,868.67
O–H	3,469.9	3,304.08	3,474.76
O–H	3,304.08	–	–
N–H	3,065.90	3,067.36	3,065.90
CH ₂	2,925.12	2,924.12	2,923.67
CH ₂	2,853.28	–	–
O–H	2,513.86	–	–
C≡C	2,108.87	2,094.40	2,110.79
C=O	1,652.28	1,656.4	1,656.62
N–H and C–N	1,543.80	1,546.21	1,547.66
CH ₃ and CH ₂	1,401.09	1,401.09	1,401.7
C–N and N–H	1,241.98	1,240.05	1,242.57
P–O	1,032.74	1,033.22	1,033.70
PO ₄ ^{3–}	561.21	562.65	559.76

Table 4. Elemental analysis of *Stolephorus* sp. powder at 3 milling times

Element	Weight [%]		
	8 h <i>M</i> ± <i>SD</i>	12 h <i>M</i> ± <i>SD</i>	24 h <i>M</i> ± <i>SD</i>
C	0.90 ± 0.19	1.22 ± 0.08	0.81 ± 0.04
N	1.35 ± 0.01	1.53 ± 0.01	0.89 ± 0.17
O	0.54 ± 0.10	0.59 ± 0.18	0.37 ± 0.11
Na	0.16 ± 0.09	0.17 ± 0.08	0.13 ± 0.09
Mg	0.06 ± 0.01	0.07 ± 0.01	0.05 ± 0.01
Al	0.07 ± 0.01	0.10 ± 0.02	0.07 ± 0.02
P	0.12 ± 0.02	0.13 ± 0.04	0.09 ± 0.03
S	0.09 ± 0.01	0.10 ± 0.02	0.07 ± 0.02
Cl	0.23 ± 0.12	0.33 ± 0.23	0.20 ± 0.14
K	0.12 ± 0.01	0.14 ± 0.03	0.09 ± 0.02
Ca	0.20 ± 0.03	0.23 ± 0.06	0.15 ± 0.05
Ca/P ratio	1.68 ± 0.09	1.82 ± 0.16	1.72 ± 0.05

**Fig. 4.** Scanning electron microscopy–energy dispersive spectroscopy (SEM-EDS) images of *Stolephorus* sp. powder at 3 milling times

A. 8 h (×200 magnification); B. 12 h (×200 magnification); C. 24 h (×200 magnification); D. 8 h (×1,000 magnification); E. 12 h (×1,000 magnification); F. 24 h (×1,000 magnification).

Table 5. Comparison of protein and mineral composition of *Stolephorus* sp. powder before and after milling

Substance	Initial (microscale)	8 h	12 h	24 h
Protein [%]	64.50	61.31	59.72	54.11
Sodium [mg/kg]	7,420	7,382	7,115	6,956
Calcium [mg/kg]	28,912	28,876	28,751	27,318
Magnesium [mg/kg]	1,924	1,918	1,877	1,843

Discussion

The examination identified 18 amino acids and demonstrated high protein and mineral scores (Table 1). The results surpassed the findings of the previous study¹³ due to a different sample preparation method. The previous study used fresh fish as a sample, whereas this study used the dried fish powder. This type of research has never been published before, as previous research has focused on the reduction of the size of fish bones, not the entire fish. In addition, this study used a different type of fish (snakehead) and employed calcination in a furnace prior to ball milling.⁹ The previous study achieved a reduction in size to 38.9445 nm.⁹ However, this technique is unsuitable for use with whole fish, because the protein is damaged by the calcination process. In this research, the FTIR test revealed the presence of proteins and organic compounds across the 8-, 12- and 24-h milling results, indicating no significant difference in pattern.

The amino acid content of the samples is beneficial for cell maintenance and repair, which is crucial for dental pulp tissue. Dental pulp tissue is surrounded by hard tissue, making it more susceptible to cell death when injured.¹⁴ Studies on the roles of amino acids in cells are widespread in the medical field, but they are less prevalent in dentistry. Previous studies have demonstrated the importance of amino acids, such as valine, in the proliferation and maintenance of hematopoietic stem cells (HSCs). Human HSCs are unable to proliferate in valine-depleted conditions.¹⁵ Another study described threonine as a nutritional modulator that influences the immune system via the mitogen-activated protein kinase and the target of the rapamycin signal pathway.¹⁶ Methionine functions as a reactive oxygen species scavenger and a crucial player in the oxidative stress response.¹⁷ Aspartate reduces doxorubicin toxicity in *Streptomyces cerevisiae* by providing carbon to the tricarboxylic acid cycle, and the addition of aspartate increases cell survival by promoting mitochondrial activity. The same effect can be achieved by the addition of asparagine, glutamate, glutamine, alanine, serine, lysine, and methionine.¹⁸ Based on these studies, it can be stated that the *Stolephorus* sp. powder, a source of protein and amino acids, has great potential to promote cell repair.

Calcium ions were detected at a high level in the sample. These ions are established as second messengers in many cellular activities, whereby they regulate intracellular signals. A previous study demonstrated that calcium is beneficial in cell recruitment and regeneration.¹⁹ These ions upregulate the expression of multiple cytokines in progenitor cells and have an influence on the extracellular signal of the calcium-sensing receptor. Receptor activation affects the chemotactic response of mesenchymal stem cells (MSCs) to calcium.¹⁹ Calcium escalation has also been reported to cause cell proliferation and enhance the expression of osteopontin, inducing matrix mineralization of MSCs.²⁰ According to these findings, it can be posited that the *Stolephorus* sp. powder, as a natural calcium source, may promote bone and dentin regeneration.

These findings elucidate the results of various studies on *Stolephorus* sp. The daily intake of *Stolephorus* sp. has been demonstrated to increase the number of osteocytes and the mandibular alveolar bone density in Wistar rats.⁵ Another study has shown that the application of *Stolephorus* sp. extract on dental pulp perforation increased the number of odontoblasts. Odontoblasts are responsible for the formation of dentin.⁶

The delivery of active pharmaceutical ingredients (APIs) is an important area of research. Particle size reduction has an impact on accelerating this process. Particle size reduction treatment increases the surface area, as well as the solubility and bioavailability of APIs.^{21,22} Nanoscale particles are attained by a top-down or bottom-up approach.^{23,24} The nanoscale range is 1–1,000 nm,²⁵ although some experts restrict it to <100 nm.

This study employed the top-down approach using high-energy ball milling. High-energy ball milling is a technique in which a powdered sample and grinding balls are placed in a container and subjected to a rotational motion. Two categories were identified within the process: mechanical alloying (MA); and mechanical disordering (MD). In MA, the elements of the powder are fractured and rewelded within a high-energy ball mill. In MD, the crystalline structure undergoes a transition to an amorphous state without altering its elemental composition.²⁶ Zirconia grinding balls were chosen due to their high density, hardness and toughness.

The results of this experiment demonstrated that the ball-milling process reduced the particle size of *Stolephorus* sp. powder from the microscale to the nanoscale. The duration of milling has an impact on the particle size and the polydispersity index. Although the PSA results indicated that 8 h of milling resulted in the smallest particle dimensions (463.3 ± 105.7 nm), the SEM image of the powder milled for 8 h showed the roughest size distribution of particles. The 24-h milling powder occupied the second place (789.3 ± 170.7 nm) and displayed the most uniform size distribution of particles in the SEM image. In addition to the average particle size, the PSA showed the polydispersity index of the samples.

The polydispersity index ranges between 0.0 (monodisperse particle size) and 1.0 (multidisperse particle size).²⁷ The measurement of the 12-h milling powder showed the most significant particles among the remaining samples (1,365.4 nm), yet exhibited the lowest polydispersity index. The PSA tools used in the study operated based on the dynamic light scattering technique. A polydispersity index exceeding 0.7 indicates a broad size distribution of the sample.²⁸

The SEM images showed that the particle size reduction process induced agglomeration (Fig. 4). Agglomeration can be attributed to the adhesion of particles due to the presence of weak forces, which ultimately results in the formation of a cluster of particles. Previous studies that used dry milling also documented this phenomenon.^{29,30} Agglomeration obscured the PSA results. Thus, the findings should be confirmed by another method.³¹

The EDS analysis identified the presence of major elements (carbon, oxygen and nitrogen), known as protein composers.³² This finding is also corroborated by the FTIR results, which revealed the presence of hydroxyl, N–H and CH₂ functional groups within the same spectral range as those reported in the previous studies.^{33,34} Moreover, the other functional groups (CH₃, C–N and N–H), known as protein composers, were detected in areas that have been previously confirmed by other studies.^{35,36}

The EDS examination revealed the presence of calcium and phosphorus, which originated from the scales and bones of *Stolephorus* sp.^{37,38} The FTIR results showed asymmetrical stretching and P–O bands, which aligned with the findings of the previous studies.^{33–35} The Ca/P ratios obtained from the elemental examination were compared to the HAp stoichiometry (1.67). According to multiple comparisons in the statistical analysis using one-way ANOVA, 24-h milling powder was found to be almost stoichiometric in nature. However, no significant difference was observed between the 3 groups. Hydroxyapatite is used in bone and dentin regeneration studies due to its chemical similarities with natural bones.^{39,40} The compound facilitates osteoinduction, osteoconduction, osseointegration, remineralization, and dental pulp repair.^{41–43}

The FTIR results for the *Stolephorus* sp. powder at different milling times showed an insignificant difference in transmittance and wavenumber. Therefore, the milling time did not influence the alteration of the functional group compounds. The peaks observed in the wavenumbers of 8-, 12- and 24-h milling samples, as illustrated in the wavenumber area of $3,869.15$ – $3,304.08$ cm⁻¹, indicate the presence of functional groups of O–H compounds, and are indicative of the presence of hydroxyl functional groups in fish protein. On the other hand, the wavenumbers of $3,065.90$ cm⁻¹ and $3,067.36$ cm⁻¹ show the vibration of the N–H compound group. Furthermore, the wavenumber area between $2,925.12$ cm⁻¹ and $2,853.28$ cm⁻¹ represents the functional group of the CH₂

compound. The wavenumber area between 2,110.79 cm^{-1} and 2,108.87 cm^{-1} indicates the stretching of the functional groups of the $\text{C}\equiv\text{C}$ compounds. With regard to the wavenumber areas of 1,656.62 cm^{-1} , 1,656.14 cm^{-1} and 1,652.28 cm^{-1} , they show sharp and prominent peaks, representing the functional groups of the $\text{C}=\text{O}$ compounds derived from fish protein. Previous studies have also revealed that the FTIR spectrum of protein present in fish exhibits peaks at 3,304–3,315 cm^{-1} , 2,922–2,940 cm^{-1} , 1,600–1,700 cm^{-1} , 1,550–1,600 cm^{-1} , and 1,220–1,320 cm^{-1} .^{33,34} The results of this study are consistent with the results of the synthesis that has been carried out.^{33,34} Furthermore, the area of 1,401.57–1,401.09 cm^{-1} represents the functional groups (CH_3 and CH_2) that constitute proteins.³⁶ The wavenumbers of 1,242.57 cm^{-1} , 1,240.05 cm^{-1} and 1,241.98 cm^{-1} show the protein's functional groups of $\text{C}-\text{N}$ and $\text{N}-\text{H}$ constituents.³⁵ The 3 powders also showed strong absorption peaks at approx. 1,032.74 cm^{-1} , 1,033.22 cm^{-1} and 1,033.70 cm^{-1} , which were marked by the asymmetric stretching of the phosphate group ($\text{P}-\text{O}$).³⁵ The more visible peaks or bands at 561.21 cm^{-1} , 562.65 cm^{-1} and 559.76 cm^{-1} correspond to PO_4^{3-} residues from fish samples.^{33,42}

Although the milling process can change the protein and mineral content, its influence was not significant in this study (Table 5). The high-energy milling process generates heat, which can alter the material's physicochemical properties. They can be influenced by speed, milling time, moisture content, pre-treatment process, type of ball mill pot, ball size, proportion of pot filling, and other factors.^{44,45} Therefore, to minimize the reduction in protein content, the milling procedure was performed with a pot volume of 55%, at a low speed and with a large ball size. According to previous studies, this process can decrease the size of protein particles, reduce the temperature rise and maintain the physicochemical properties of the product.^{44–47} Thus, in our study, there was a decrease in the protein and mineral content from baseline to the longest grinding time. However, the observed difference was not significant. This finding is consistent with the results of previous research.^{46,47}

Conclusions

The findings of this study lay the foundation for future research using *Stolephorus* sp. as an inducer of dental pulp cell repair. Further research will continue to develop vital pulp therapy using nanosized materials derived from *Stolephorus* sp. In addition, in vivo tests will be conducted to evaluate the formation and quality of reparative dentin induced in pulp perforation. The high mineral and protein content can be maintained throughout the particle size reduction process. A reduction in the particle size enhances bioavailability and accelerates the recuperation time.

Ethics approval and consent to participate

Not applicable.

Data availability


The datasets generated and/or analyzed during the current study are available from the corresponding author on reasonable request.


Consent for publication

Not applicable.

ORCID iDs

Anastasia Elsa Prahasti  <https://orcid.org/0000-0003-2709-5081>

Tamara Yuanita  <https://orcid.org/0000-0002-5320-7772>

Retno Pudji Rahayu  <https://orcid.org/0000-0003-4429-3653>

References

- Atanasov AG, Zotchev SB, Dirsch VM, Supuran CT; International Natural Product Sciences Taskforce. Natural products in drug discovery: Advances and opportunities. *Nat Rev Drug Discov.* 2021;20(3):200–216. doi:10.1038/s41573-020-00114-z
- Prahasti AE, Yuanita T. Utilization of anchovy in dentistry. *Malaysian J Med Health Sci.* 2021;17(Suppl6):87–90. <https://repository.unair.ac.id/123692>. Accessed August 16, 2023.
- Rauf FH, Tangke U, Namsa D. Dinamika Populasi Ikan Teri (*Stolephorus* sp) yang di Daratkan di Pasar Higienis Kota Ternate. *J Biol Sains Teknol.* 2019;1(1):1–9. doi:10.52046/biosainstek.v1i01.206.1-9
- Safyanti, Andrafikar. Efficacy of micronutrient supplementation from local food of bada fish (*Stolephorus insularis*) on the status of anemia among adolescents in Padang city. *KnE Life Sci.* 2019;2019:111–115. doi:10.18502/kl.v4i15.5744
- Astrina I, Primasari A, Keumalasari D. Anchovy intake to increase alveolar bone density of the mandibles in white wistar rats (*Rattus norvegicus*). *IOSR J Dent Med Sci.* 2018;17(3):28–33. doi:10.9790/0853-1703092833
- Effendi MC, Alrista R, Taufiq A, Susanto H. Effects of anchovy (*Stolephorus* sp.) hydroxyapatite on the number of odontoblast cells for reparative dentine stimulation on *Rattus norvegicus* teeth. *AIP Conf Proc.* 2021:1–7. doi:10.1063/5.0052863
- MacDonell R, Hamrick MW, Isales CM. Protein/amino-acid modulation of bone cell function. *Bonekey Rep.* 2016;5:827. doi:10.1038/bonekey.2016.58
- Sari RP, Revianti S, Nugroho HK. Application direct pulp capping *Stolephorus insularis* cream to dentin Reparatif. In: Kalanjati VP, ed. *The Future of Anatomy. 6th Asia Pacific International Congress of Anatomy.* 2011:134–137. <https://dspace.hangtuah.ac.id/xmlui/bitstream/handle/dx/1033/APICA%202011.pdf?sequence=3&isAllowed=y>. Accessed August 16, 2023.
- Muryati M, Hariani PL, Said M. Preparation and characterization nanoparticle calcium oxide from snakehead fish bone using ball milling method. *Indones J Fundamental Appl Chem.* 2019;4(3):111–115. doi:10.24845/ijfac.v4.i3.111
- Hoshyar N, Gray S, Han H, Bao G. The effect of nanoparticle size on in vivo pharmacokinetics and cellular interaction. *Nanomedicine (Lond).* 2016;11(6):673–692. doi:10.2217/nnm.16.5
- Mæhre HK, Dalheim L, Edvinsen GK, Elvevoll EO, Jensen IJ. Protein determination – method matters. *Foods.* 2018;7(1):5. doi:10.3390/foods7010005
- Zhang H, Baeyens J, Kang Q. Measuring suspended particle size with high accuracy. *Int J Petrochem Sci Eng.* 2017;2(6):2–7. doi:10.15406/ipcse.2017.02.00058
- Sankar TV, Anandan R, Mathew S, et al. Chemical composition and nutritional value of Anchovy (*Stolephorus commersonii*) caught from Kerala coast, India. *Eur J Exp Biol.* 2013;3(1):85–89.

14. Rombouts C, Giraud T, Jeanneau C, About I. Pulp vascularization during tooth development, regeneration, and therapy. *J Dent Res*. 2017;96(2):137–144. doi:10.1177/0022034516671688
15. Taya Y, Ota Y, Wilkinson AC, et al. Depleting dietary valine permits nonmyeloablative mouse hematopoietic stem cell transplantation. *Science*. 2016;354(6316):1152–1155. doi:10.1126/science.aag3145
16. Tang Q, Tan P, Ma N, Ma X. Physiological functions of threonine in animals: Beyond nutrition metabolism. *Nutrients*. 2021;13(8):2592. doi:10.3390/nu13082592
17. Campbell K, Vowinkel J, Keller MA, Ralser M. Methionine metabolism alters oxidative stress resistance via the pentose phosphate pathway. *Antioxid Redox Signal*. 2016;24(10):543–547. doi:10.1089/ars.2015.6516
18. Dornfeld K, Madden M, Skildum A, Wallace KB. Aspartate facilitates mitochondrial function, growth arrest and survival during doxorubicin exposure. *Cell Cycle*. 2015;14(20):3282–3291. doi:10.1080/15384101.2015.1087619
19. Aquino-Martínez R, Angelo AP, Pujol FV. Calcium-containing scaffolds induce bone regeneration by regulating mesenchymal stem cell differentiation and migration. *Stem Cell Res Ther*. 2017;8(1):265. doi:10.1186/s13287-017-0713-0
20. Lee MN, Hwang HS, Oh SH, et al. Elevated extracellular calcium ions promote proliferation and migration of mesenchymal stem cells via increasing osteopontin expression. *Exp Mol Med*. 2018;50(11):1–16. doi:10.1038/s12276-018-0170-6
21. Khadka P, Ro J, Kim H, et al. Pharmaceutical particle technologies: An approach to improve drug solubility, dissolution and bioavailability. *Asian J Pharm Sci*. 2014;9(6):304–316. doi:10.1016/j.ajps.2014.05.005
22. Afifi SA, Hassan MA, Abdelhameed AS, Elkhodairy KA. Nanosuspension: An emerging trend for bioavailability enhancement of etodolac. *Int J Polym Sci*. 2015;2015:11–15. doi:10.1155/2015/938594
23. Salazar J, Müller RH, Möschwitzer JP. Combinative particle size reduction technologies for the production of drug nanocrystals. *J Pharm (Cairo)*. 2014;2014:265754. doi:10.1155/2014/265754
24. Mageswari A, Srinivasan R, Subramanian P, Ramesh N, Gothandam KM. Nanomaterials: Classification, Biological Synthesis and Characterization. In: Ranjan S, Dasgupta N, Lichtfouse E, eds. *Nanoscience in Food and Agriculture* 3. 3rd ed. 2016:31–71. doi:10.1007/978-3-319-48009-1
25. Rogers B, Adams J, Pennathur S. Introduction to Miniaturization. In: *Nanotechnology*. 3rd ed. Boca Raton, FL: CRC Press; 2015:51–76. doi:10.1201/b17424-6
26. Sherif El-Eskandarany M, Al-Hazza A, Al-Hajji LA, et al. Mechanical milling: A superior nanotechnological tool for fabrication of nanocrystalline and nanocomposite materials. *Nanomaterials*. 2021;11(10):2484. doi:10.3390/nano11102484
27. Danaei M, Dehghankhold M, Ataei S, et al. Impact of particle size and polydispersity index on the clinical applications of lipidic nanocarrier system. *Pharmaceutics*. 2018;10(2):57. doi:10.3390/pharmaceutics10020057
28. Stetefeld J, McKenna SA, Patel TR. Dynamic light scattering: A practical guide and applications in biomedical sciences. *Biophys Rev*. 2016;8(4):409–427. doi:10.1007/s12551-016-0218-6
29. Guzzo PL, Marinho de Barros FB, Soares BR, Santos JB. Evaluation of particle size reduction and agglomeration in dry grinding of natural quartz in a planetary ball mill. *Powder Technol*. 2020;368:149–159. doi:10.1016/j.powtec.2020.04.052
30. Blanc N, Mayer-Laigle C, Frank X, Radjai F, Delenne JY. Evolution of grinding energy and particle size during dry ball-milling of silica sand. *Powder Technol*. 2020;376:661–667. doi:10.1016/j.powtec.2020.08.048
31. Gosens I, Post JA, de la Fonteyne LJJ, et al. Impact of agglomeration state of nano- and submicron sized gold particles on pulmonary inflammation. *Part Fibre Toxicol*. 2010;7(1):37. doi:10.1186/1743-8977-7-37
32. van Goudoever JB, Vlaardingerbroek H, van den Akker CH, de Groof F, van der Schoor SRD. Amino acids and proteins. *World Rev Nutr Diet*. 2014;110:49–63. doi:10.1159/000358458
33. Zhang Y, Tu D, Shen Q, Dai Z. Fish scale valorization by hydrothermal pretreatment followed by enzymatic hydrolysis for gelatin hydrolysate production. *Molecules*. 2019;24(16):2998. doi:10.3390/molecules24162998
34. Riaz T, Zeeshan R, Zarif F, et al. FTIR analysis of natural and synthetic collagen. *Appl Spectrosc Rev*. 2018;53(9):703–746. doi:10.1080/05704928.2018.1426595
35. Sasmal P, Begam H. Extraction of type-I collagen from sea fish and synthesis of hap/collagen composite. *Procedia Mater Sci*. 2014;5:1136–1140. doi:10.1016/j.mspro.2014.07.408
36. Hernández-Martínez M, Gallardo-Velázquez T, Osorio-Revilla G, Almaraz-Abarca N, Ponce-Mendoza A, Vásquez-Murrieta MS. Prediction of total fat, fatty acid composition and nutritional parameters in fish fillets using MID-FTIR spectroscopy and chemometrics. *LWT – Food Sci Technol*. 2013;52(1):12–20. doi:10.1016/j.lwt.2013.01.001
37. Amaral Corrêa TH, França Holanda JN. Fish bone as a source of raw material for synthesis of calcium phosphate. *Mater Res*. 2019;22(Suppl 1):e20190486. doi:10.1590/1980-5373-MR-2019-0486
38. Granito RN, Renno ACM, Yamamura H, de Almeida MC, Ruiz PLM, Ribeiro DA. Hydroxyapatite from fish for bone tissue engineering: A promising approach. *Int J Mol Cell Med*. 2018;7(2):80–90. doi:10.22088/IJCM.BUMS.7.2.80
39. Kattimani VS, Kondaka S, Lingamaneni KP. Hydroxyapatite – past, present, and future in bone regeneration. *Bone Tissue Regener Insights*. 2016;7:S36138. doi:10.4137/btri.s36138
40. Von Euw S, Wang Y, Laurent G, et al. Bone mineral: New insights into its chemical composition. *Sci Rep*. 2019;9(1):1–11. doi:10.1038/s41598-019-44620-6
41. Sathiyavimal S, Vasantharaj S, LewisOscar F, Selvaraj R, Brindhadevi K, Pugazhendhi A. Natural organic and inorganic – hydroxyapatite biopolymer composite for biomedical applications. *Prog Org Coat*. 2020;147:105858. doi:10.1016/j.porgcoat.2020.105858
42. Shi P, Liu M, Fan F, Yu C, Lu W, Du M. Characterization of natural hydroxyapatite originated from fish bone and its biocompatibility with osteoblasts. *Mater Sci Eng C Mater Biol Appl*. 2018;90:706–712. doi:10.1016/j.msec.2018.04.026
43. Okamoto M, Matsumoto S, Sugiyama A, et al. Performance of a biodegradable composite with hydroxyapatite as a scaffold in pulp tissue repair. *Polymers (Basel)*. 2020;12(4):937. doi:10.3390/POLYM12040937
44. Schmidt R, Martin Scholze H, Stolle A. Temperature progression in a mixer ball mill. *Int J Ind Chem*. 2016;7(2):181–186. doi:10.1007/s40090-016-0078-8
45. Tharanon W, Peerapattana J. The effects of ball mill processing on the physicochemical properties of glutinous rice starch. *Thai J Pharm Sci*. 2020;44(2):91–8. <https://www.thaiscience.info/Journals/Article/TJPS/10996283.pdf>. Accessed August 19, 2024.
46. Wang Z, Chang S, Li Y, et al. Effects of ball milling treatment on physicochemical properties and digestibility of Pacific oyster (*Crassostrea gigas*) protein powder. *Food Sci Nutr*. 2018;6(6):1582–1590. doi:10.1002/fsn3.705
47. Chen X, Guo M, Sang Y, Sun J. Effect of ball-milling treatment on the structure, physicochemical properties and allergenicity of proteins from oyster (*Crassostrea gigas*). *LWT*. 2022;166:113803. doi:10.1016/j.lwt.2022.113803